HHS Public Access

Author manuscript

Cancer Immunol Res. Author manuscript; available in PMC 2017 June 01.

Published in final edited form as:

Cancer Immunol Res. 2016 June ; 4(6): 474–480. doi:10.1158/2326-6066.CIR-15-0213.

Myelodysplastic Syndrome Revealed by Systems Immunology in a Melanoma Patient Undergoing Anti–PD-1 Therapy

Allison R. Greenplate[1,2], **Douglas B. Johnson**[3], **Mikael Roussel**[2,4], **Michael R. Savona**[3], **Jeffrey A. Sosman**[3], **Igor Puzanov**[3], **P. Brent Ferrell**[#2,3], and **Jonathan M. Irish**[#1,2]

[1]Department of Pathology, Microbiology, and Immunology, Vanderbilt University Medical Center, Nashville, TN.

[2]Department of Cancer Biology, Vanderbilt University, Nashville, TN, USA.

[3]Department of Medicine, Vanderbilt University Medical Center, Nashville, TN.

[4]Laboratoire d'Hématologie, Pôle Cellules et Tissus, CHU, INSERM UMR 917, Rennes, France

[#] These authors contributed equally to this work.

Abstract

Antibodies aimed at blocking the interaction between programmed cell death-1 (PD-1) and its ligands have shown impressive efficacy in a variety of malignancies and are generally well tolerated. Research has focused intensely on T cells and their interaction with cells within melanoma tumors, while relatively little is understood about the systems immunology of the cells in the blood during checkpoint inhibitor therapy. Longitudinal cytomic analysis using mass cytometry can characterize all the cells in a small sample of blood and has the potential to reveal key shifts in the cellular milieu occurring during treatment. We report a case of advanced melanoma in which mass cytometry detected abnormal myeloid cells resulting from myelodysplastic syndrome (MDS) in the blood following treatment with an anti–PD-1 agent. Myeloid blasts comprised <1% of peripheral blood mononuclear cells (PBMC) one month after the start of treatment. By 6 months after starting therapy, myeloid blasts comprised 5% of PBMC and a bone marrow biopsy confirmed refractory anemia with excess blasts-2 (RAEB-2). Longitudinal mass cytometry immunophenotyping comprehensively characterized blast phenotype evolution and revealed elevated PD-1 expression on the surface of non-blast myeloid cells. These findings highlight the clinical significance of cytomic monitoring, indicate that the myeloid compartment should be monitored during checkpoint inhibitor therapy, and emphasize the value of systems immunology in medicine.

Keywords

Immunotherapy; mass cytometry; systems immunology; myelodysplastic syndrome; melanoma

Corresponding authors: Dr. Jonathan M. Irish Ph.D., Assistant Professor of Cancer Biology, Vanderbilt University School of Medicine, 740B Preston Building, 2220 Pierce Avenue, Nashville, TN 37232-6840; Tel (615) 875-0965; ; Email: jonathan.irish@vanderbilt.edu, P. Brent Ferrell, Jr., MD, Instructor in Medicine, Vanderbilt University Medical Center, 777 Preston Research Building, 2220 Pierce Avenue, Nashville, TN 37232-6840; Tel (615) 875-8619; ; Email: brent.ferrell@vanderbilt.edu

Conflict-of-interest disclosure: JMI declares a competing financial interest (co-founder and board member, Cytobank Inc.). JAS reports consulting for Merck and receiving research funding from Bristol-Myers Squibb and GlaxoSmithKline.

Introduction

Antibodies targeting the programmed cell death-1 (PD-1) receptor and its ligand (PD-L1) have demonstrated remarkable activity in a variety of solid tumor malignancies and Hodgkin disease ([1-5]). Agents such as nivolumab and pembrolizumab block this key immune checkpoint to generate effective $CD8^+$ T cell–mediated antitumor immune responses ([6]). Although generally well-tolerated, anti–PD-1/PD-L1 agents have also induced grade 3–4 immune-mediated adverse events (~5% of patients) ([1, 3, 7]). The ability to monitor the immune system as a whole is needed in clinical settings where therapies are designed to alter the interaction between multiple cell types, such as the blockade of the PD-1/PD-L1 interaction. Mass cytometry has emerged as an important platform for comprehensive and minimally biased immune profiling ([8]). This approach has been applied effectively in the context of healthy human bone marrow, blood, and tonsil tissue ([9-12]). An important element of high dimensional mass cytometry is the use of unsupervised computational data analysis tools that reveal and characterize cells with unusual phenotypes ([13-15]).

To examine the effects of immune checkpoint inhibition on peripheral blood cell subsets, we performed serial blood acquisition in patients with advanced melanoma being treated with pembrolizumab. Multiplexed mass cytometry analysis of peripheral blood characterized the phenotypic evolution of all major immune cell and blast populations. Here, we present a case report of a single patient from this study who experienced clinical emergence and progression of MDS while undergoing treatment with pembrolizumab.

Patients, Materials, & Methods

Subject

The subject gave consent to an IRB-approved research protocol to collect serial blood prior to treatment (baseline) and following pembrolizumab (at 3 weeks, 6 weeks, 12 weeks, and 24 weeks). Peripheral blood was obtained during regularly scheduled laboratory blood draws in accordance with the Declaration of Helsinki following protocols approved by Vanderbilt University Medical Center (VUMC) Institutional Review Board.

PBMC preparation

Peripheral blood mononuclear cells (PBMCs) were isolated from 20 mL of freshly drawn blood using sodium heparin anticoagulant and Ficoll-Paque PLUS (GE Healthcare Bio-sciences, Uppsala, Sweden) centrifugation. Freshly isolated PBMCs were immediately cryopreserved in FBS (Life Technologies, Grand Island, NY, USA) containing 12% DMSO (Fischer Scientific, Fair Lawn, NJ, USA).

Mass cytometry

Purified antibodies from Biolegend (San Diego, CA, USA) were labeled using MaxPar DN3 kits (Fluidigm Sciences, Toronto, Canada) and stored at 4°C in antibody stabilization buffer (Candor Bioscience GmbH, Wangen, Germany). PBMC were first incubated with a viability reagent (25 μM cisplatin, Enzo Life Sciences, Farmingdale, NY, USA) as previously

described ([16]). For staining, 2×10^6 cells were washed in PBS containing 1% BSA and stained in 50 μL PBS/1% BSA containing antibody cocktail. Cells were stained for 30 minutes at room temperature using antibodies listed (**Supplementary Table S1**). Cells were washed twice in PBS/1% BSA and then fixed with 1.6% paraformaldehyde (PFA, Electron Microscopy Sciences, Hatfield, PA, USA). Cells were washed once in PBS and permeabilized by resuspending in ice cold methanol. After incubating overnight at −20°C, cells were washed twice with PBS/1% BSA and stained with iridium DNA intercalator (Fluidigm Sciences,) for 30 minutes at room temperature. Finally, cells were washed twice with PBS and twice with deionized water before being resuspended in 1× EQ™ Four Element Calibration Beads (Fluidigm Sciences) according to the manufacturer's instructions and collected on a CyTOF 1.0 mass cytometer (Fluidigm Sciences) at the Vanderbilt Flow Cytometry Shared Resource. Events were normalized prior to analysis.

Cytometry data analysis

Analysis was performed on Cytobank using published techniques including viSNE ([13, 17]). Each file was pregated on $CD45^{lo}$ events. All $CD45^{lo}$ events were used and BTLA, CD69, HLA-DR, CD45RO, CD44, CD27, CD3, CD45RA, CXCR3, CD33, CD16, PD-L1, CD4, CD8a, CD43, ICOS, CD20, CD38, CCR4, CD45, CCR7, CD25, CXCR5, CD57, PD-1, and CD56 were used to create the t-SNE axes of the viSNE map. NK cells were gated as $CD16^{+}CD3^{-}CD19^{-}HLA\text{-}DR^{-}$ to allow consistent gating between this study and other immune monitoring studies where CD56 is not available. For this patient, equivalent NK cell frequencies were observed with and without inclusion of CD56 in the gating scheme.

Results

Case report

A 72-year-old female patient with a past medical history of breast cancer treated with mastectomy and chemotherapy (24 years prior) developed swelling in her thigh. CT scan showed a 2×4×3 cm complex, cystic mass in the soft tissues of the thigh. She underwent a resection that revealed melanoma with involved lateral margins. No primary site was identified, and she received 2800 cGy via external beam therapy to the resection margin in the thigh (American Joint Committee on Cancer [AJCC] stage TxNxM1a). A surveillance PET-CT scan performed 18 months later demonstrated multiple new pulmonary nodules, and she received ipilimumab 3 mg/kg for four doses. Repeat CT scan showed disease progression in the lungs, and she was started on pembrolizumab 2 mg/kg every 3 weeks (pembrolizumab expanded access program). Her initial surveillance scans in 3 months showed a mixed response in lung nodules but overall stable disease. Her subsequent CT scan 6 months into therapy confirmed disease progression, primarily in two lung nodules (**Fig. 1A**). She underwent radiation to those nodules and has continued pembrolizumab.

Prior to starting pembrolizumab, the patient was noted to have mild thrombocytopenia (platelet count 95×10^9/L), which had been present but stable for the previous 18 months, and normal white blood cell count and hemoglobin. Her monocyte count was slightly elevated (1.27×10^9/L), but otherwise she had a normal differential. One month after starting pembrolizumab, she developed a clinically detectable but small circulating myeloid

blast population on her CBC differential that remained at < 1% for the next two months (**Fig. 1B**). Blasts were not detected in her pretreatment sample on her CBC differential, but were detected pretreatment by CyTOF analysis (**Fig. 2**). After treatment, her peripheral blast percentage rose to 4.4% and her platelets and hemoglobin fell to 72×10^9/L and 9.4 g/dL, respectively, prompting a bone marrow biopsy. This revealed refractory anemia with excess blasts-2 (RAEB-2) with 8.5% blasts. During this workup, her peripheral blast percentage ranged from 7-11% and she began decitabine treatment. Since initiating decitabine, she has felt well and her peripheral blast count has stabilized.

High Dimensional Cytometry Revealed Peripheral Blasts

Samples of peripheral blood from prior to anti–PD-1 therapy, 3 weeks, 12, and 6 months following the initiation of therapy were analyzed by a 33-parameter mass cytometry panel. Major cell populations were revealed using traditional biaxial plots (**Fig. 2**). As a subset of peripheral blood mononuclear cells (PBMCs), blasts ranged in abundance from 1.16% pre-therapy to 4.65% at six months after the start of treatment (**Fig. 2A** and **Fig. 2C**, left). In comparison to mature myeloid and monocyte cell populations, the majority of peripheral blasts expressed lower CD45 and CD33, higher CD38, and comparable HLA-DR (**Fig. 2B**). Four additional cell populations were monitored using mass cytometry over the course of anti–PD-1 therapy (**Fig. 2C** right).

Myeloid cells ($HLA\text{-}DR^+CD19^-CD3^-CD16^-$) increased over the course of anti–PD-1 therapy, while T cells ($CD3^+CD19^-$), B cells ($CD19^+CD3^-$), and NK cells ($CD16^+CD3^-CD19^-HLA\text{-}DR^-$) decreased.

Increased percent of PD-1$^+$ monocytes during therapy

To determine which cells could be modulated by pembrolizumab, mass cytometry was used to monitor PD-1 protein expression on all major peripheral blood subsets. In the blood of healthy donors, 1.8% ± 0.68% of $HLA\text{-}DR^{pos}CD19^{neg}CD3^{neg}CD16^{neg}$ myeloid lineage PBMCs expressed PD-1 ($n = 5$). In contrast, elevated levels PD-1^+ myeloid cells were seen in all pre- and post-treatment samples collected from the melanoma patient (**Fig. 3A**). PD-1^+ myeloid cells decreased over therapy from 4.04% pre-treatment to 2.81% at 6 months after the start of pembrolizumab. The percentage of PD-1^+ $CD4^+$ T cells in PBMC was high prior to therapy (4.93% in the patient prior to therapy *vs* 3.31% ± 1.28% in healthy donors, $n = 5$). However, by week 3 post therapy, the frequency of both PD-1^+ CD8 and CD4 T cells in PBMC decreased (1.94% and 2.29% respectively in patient 6 months after start of therapy *vs* 4.44% ± 2.15% and 3.31% ± 1.28% respectively in healthy donors, $n = 5$). B cells, NK cells, and blasts were very rarely PD-1^+ (**Fig. 3A**, < 2% PD-1^+ at all observed times).

Mass cytometry was also used to monitor expression of PD-L1, a key ligand for PD-1 and potential biomarker of anti–PD-1 treatment response ([18]). PD-L1 expression was largely absent; no cell subset was observed to express PD-L1 on >1.5% of cells (data not shown). Monocytes were the only peripheral cell subset to exhibit increased PD-1 expression and a large increase in activation marker CD45RA was seen on monocytes over the course of therapy (**Fig. 3B**) ([19]).

Evolving Blast Phenotype After Three Weeks of anti–PD-1 Therapy

To assess the phenotypic changes of blasts over the course of anti–PD-1 therapy, blast cells from each time point were gated based on immunophenotype and analyzed in a single viSNE plot (**Fig. 4A**). viSNE approximates high dimensional relationships using a two dimensional (2D) scatter plot, or map, where each dot represents a single cell ([13]). Cells close together on a viSNE map are phenotypically similar across all parameters used to make the map. Gates were used to assess the percentage of cells in the most dense regions of the viSNE map and the fold change in population frequency was compared over therapy (**Fig 4B**). Before therapy, blasts fell mostly within population 1, defined by high expression of HLA-DR, CD33, CD38, CD43, and CD44 and intermediate expression of CD45RA. By 6 months after the start of therapy the cells had shifted phenotype and largely fell into population 7, defined by expression of CXCR3 in addition to the phenotypic characteristics of population 1. Each population was distinguished by key phenotypic differences (**Fig. 4C**). Populations 3 and 5 were distinguished by a lack of HLA-DR and CD33 expression along with high expression of the T cell costimulatory molecule CD28 and the chemokine trafficking marker CXCR3, respectively. Additionally, population 6 expressed both myeloid markers (HLA-DR and CD33) and neural cell adhesion molecule (NCAM/CD56), a marker expressed on NK and neural lineage cells, as well blasts in MDS and AML ([20]).

Discussion

We report here a case study of a patient who experienced progression of MDS while undergoing anti–PD-1 therapy for advanced melanoma. Subclinical MDS was detected by mass cytometry prior to treatment and blasts became clinically apparent and progressed during treatment. Given the importance of the immune checkpoint inhibitor treatment class for melanoma and other malignancies and the unexpected nature of the emergence and progression of MDS, we described the clinical features and immune evolution of this case. As anti–PD-1 directed therapies are expected to be approved and tested in numerous malignancies, cellular response profiles of the immune system as a whole must be explored. When paired with unsupervised computational analysis tools ([13]), mass cytometry provides a complete platform for immune monitoring that effectively addresses the heterogeneity and complexity of primary tissue biopsies by revealing and characterizing known and novel cell populations.

In this case study, a population of myeloid peripheral blasts emerged and was readily detected by both computational and human expert analysis. Both complete blood counts and mass cytometry were able to identify these cells, ranging from approximately 1% to 5% of PBMC. Of interest, while no peripheral blasts were identified prior to treatment on clinical analysis, a clear population was detected by mass cytometry. Lymphocytes decreased while myeloid cells increased, indicative of disrupted hematopoiesis. Additionally, mass cytometry effectively characterized PD-1 and PD-L1 expression on all major peripheral blood immune subsets. Phenotypes of immune cells and blasts were tracked over the course of therapy, revealing an increase in $PD\text{-}1^{+}$ monocytes and the emergence of a $CXCR3^{+}$ blast population, respectively. This phenotypic evolution of peripheral blasts may be shaped by the presence of anti–PD-1, or may simply reflect the natural history of MDS.

Peripheral blasts were largely negative for PD-1 and PD-L1 protein expression underscoring the premise that if anti–PD-1 is used to treat MDS or myeloid leukemia in the future, additional treatments may be needed to augment therapy in cases where a PD-L1^{-} peripheral blast population is present ([21]). Notably, the frequency of PD-1^{+} T cells decreased following anti–PD-1 treatment. This observation might be explained by occupation or internalization of surface PD-1 mediated by pembrolizumab ([1]), natural variation over time, treatment induced changes in the blood T cell milieu, and trafficking of PD-1^{+} cells to another location, such as tumor. The presence of myeloid blasts may alter the outcome of immune checkpoint inhibitors for PD-1 expressing T cells.

In this case, it is unclear whether pembrolizumab contributed to MDS progression. Increasingly, the role of the immune system in the development and progression of MDS is being elucidated. Inflammatory cytokines and Th17-cell subsets are predominant in low risk disease, but in high risk MDS (as in our patient) regulatory subsets begin to dominate, giving rise to an overall suppressive immune microenvironment ([22], [23]). Myeloid- derived suppressor cells (MDSCs) and associated suppressive cytokines TGFβ and IL10 are increased in MDS bone marrow and may promote progression of disease and suppress normal hematopoiesis through immune suppression and dysregulation ([24]). From our data, it is clear that multiple immune regulatory processes are involved in advanced MDS and rescue of exhausted T cells through PD-1 blockade may only solve part of the problem. Perhaps inhibition of the MDSCs or cytokine responses could serve as a synergistic approach together with PD-1 blockade.

This patient is the second reported case of the development and progression of MDS while undergoing anti–PD-1 therapy ([25]). The other reported patient had Hodgkin lymphoma and received multiple prior chemotherapies. Our patient had also received both chemotherapy and radiation therapy and MDS was likely precipitated by these other factors. These cases indicate it will be valuable to monitor the myeloid compartment in anti–PD-1 treated patients.

This case study highlights both the complexity of immune monitoring in the context of cancer treatment and the power of high-dimensional tools to provide a comprehensive and minimally biased view of dynamic cellular systems. It is clear that high-dimensional immune monitoring will be of significant value in cases where immune checkpoint inhibitors are used in the context of MDS, myeloid leukemia, or other myeloid bone marrow failure syndromes. These results also underscore the critical need to characterize mechanisms of response to immune checkpoint inhibitors, as these mechanisms may depend greatly on the disease context in which they are applied.

Supplementary Material

Refer to Web version on PubMed Central for supplementary material.

Acknowledgments

Funding sources: This study was supported by NIH/NCI R00 CA143231-03 (J.M.I. and A.R.G.), F31 CA199993 (A.R.G.), K12 CA090625 (P.B.F. and D.B.J.), and the Vanderbilt-Ingram Cancer Center (VICC, P30 CA68485). ACS Melanoma Professorship (JAS)

References

1. Topalian SL, Hodi FS, Brahmer JR, Gettinger SN, Smith DC, McDermott DF, et al. Safety, activity, and immune correlates of anti-PD-1 antibody in cancer. The New England journal of medicine. 2012; 366:2443–54. [PubMed: 22658127]
2. Hamid O, Robert C, Daud A, Hodi FS, Hwu WJ, Kefford R, et al. Safety and Tumor Responses with Lambrolizumab (Anti-PD-1) in Melanoma. The New England journal of medicine. 2013; 369:134–44. [PubMed: 23724846]
3. Ribas A, Puzanov I, Dummer R, Schadendorf D, Hamid O, Robert C, et al. Pembrolizumab versus investigator- choice chemotherapy for ipilimumab-refractory melanoma (KEYNOTE-002): a randomised, controlled, phase 2 trial. The lancet oncology. 2015
4. Ansell SM, Lesokhin AM, Borrello I, Halwani A, Scott EC, Gutierrez M, et al. PD-1 Blockade with Nivolumab in Relapsed or Refractory Hodgkin's Lymphoma. The New England journal of medicine. 2014
5. Le DT, Uram JN, Wang H, Bartlett BR, Kemberling H, Eyring AD, et al. PD-1 Blockade in Tumors with Mismatch- Repair Deficiency. The New England journal of medicine. 2015; 372:2509–20. [PubMed: 26028255]
6. Chen DS, Mellman I. Oncology meets immunology: the cancer-immunity cycle. Immunity. 2013; 39:1–10. [PubMed: 23890059]
7. Herbst RS, Soria JC, Kowanetz M, Fine GD, Hamid O, Gordon MS, et al. Predictive correlates of response to the anti-PD-L1 antibody MPDL3280A in cancer patients. Nature. 2014; 515:563–7. [PubMed: 25428504]
8. Irish JM. Beyond the age of cellular discovery. Nature immunology. 2014; 15:1095–7. [PubMed: 25396342]
9. Polikowsky HG, Wogsland CE, Diggins KE, Huse K, Irish JM. Cutting Edge: Redox Signaling Hypersensitivity Distinguishes Human Germinal Center B Cells. Journal of immunology (Baltimore, Md : 1950). 2015
10. Sen N, Mukherjee G, Sen A, Bendall SC, Sung P, Nolan GP, et al. Single-cell mass cytometry analysis of human tonsil T cell remodeling by varicella zoster virus. Cell reports. 2014; 8:633–45. [PubMed: 25043183]
11. Bendall SC, Simonds EF, Qiu P, Amir el AD, Krutzik PO, Finck R, et al. Single-cell mass cytometry of differential immune and drug responses across a human hematopoietic continuum. Science (New York, NY). 2011; 332:687–96.
12. Brodin P, Jojic V, Gao T, Bhattacharya S, Angel CJ, Furman D, et al. Variation in the human immune system is largely driven by non-heritable influences. Cell. 2015; 160:37–47. [PubMed: 25594173]
13. Amir el AD, Davis KL, Tadmor MD, Simonds EF, Levine JH, Bendall SC, et al. viSNE enables visualization of high dimensional single-cell data and reveals phenotypic heterogeneity of leukemia. Nature biotechnology. 2013; 31:545–52.
14. Becher B, Schlitzer A, Chen J, Mair F, Sumatoh HR, Teng KW, et al. High-dimensional analysis of the murine myeloid cell system. 2014; 15:1181–9.
15. Diggins KE, Ferrell PB Jr. Irish JM. Methods for discovery and characterization of cell subsets in high dimensional mass cytometry data. Methods. 2015; 82:55–63. [PubMed: 25979346]
16. Fienberg HG, Simonds EF, Fantl WJ, Nolan GP, Bodenmiller B. A platinum-based covalent viability reagent for single-cell mass cytometry. Cytometry Part A : the journal of the International Society for Analytical Cytology. 2012; 81:467–75. [PubMed: 22577098]

17. Kotecha N, Krutzik PO, Irish JM. Paul Robinson J. Web-based analysis and publication of flow cytometry experiments. Current protocols in cytometry / editorial board. 2010 Chapter 10:Unit10.7.

18. Taube JM, Klein A, Brahmer JR, Xu H, Pan X, Kim JH, et al. Association of PD-1, PD-1 ligands, and other features of the tumor immune microenvironment with response to anti-PD-1 therapy. Clinical cancer research : an official journal of the American Association for Cancer Research. 2014; 20:5064–74. [PubMed: 24714771]

19. Brohee D, Higuet N. In vitro stimulation of peripheral blood mononuclear cells by phytohaemagglutinin A induces CD45RA expression on monocytes. Cytobios. 1992; 71:105–11. [PubMed: 1473353]

20. Ogata K, Nakamura K, Yokose N, Tamura H, Tachibana M, Taniguchi O, et al. Clinical significance of phenotypic features of blasts in patients with myelodysplastic syndrome. Blood. 2002; 100:3887–96. [PubMed: 12393641]

21. Ishida M, Iwai Y, Tanaka Y, Okazaki T, Freeman GJ, Minato N, et al. Differential expression of PD-L1 and PD-L2, ligands for an inhibitory receptor PD-1, in the cells of lymphohematopoietic tissues. Immunology letters. 2002; 84:57–62. [PubMed: 12161284]

22. Kordasti SY, Afzali B, Lim Z, Ingram W, Hayden J, Barber L, et al. IL-17-producing CD4(+) T cells, pro-inflammatory cytokines and apoptosis are increased in low risk myelodysplastic syndrome. Br J Haematol. 2009; 145:64–72. [PubMed: 19210506]

23. Kordasti SY, Ingram W, Hayden J, Darling D, Barber L, Afzali B, et al. CD4+CD25high Foxp3+ regulatory T cells in myelodysplastic syndrome (MDS). Blood. 2007; 110:847–50. [PubMed: 17412885]

24. Chen X, Eksioglu EA, Zhou J, Zhang L, Djeu J, Fortenbery N, et al. Induction of myelodysplasia by myeloid-derived suppressor cells. The Journal of clinical investigation. 2013; 123:4595–611. [PubMed: 24216507]

25. Ansell SM, Lesokhin AM, Borrello I, Halwani A, Scott EC, Gutierrez M, et al. PD-1 blockade with nivolumab in relapsed or refractory Hodgkin's lymphoma. The New England journal of medicine. 2015; 372:311–9. [PubMed: 25482239]

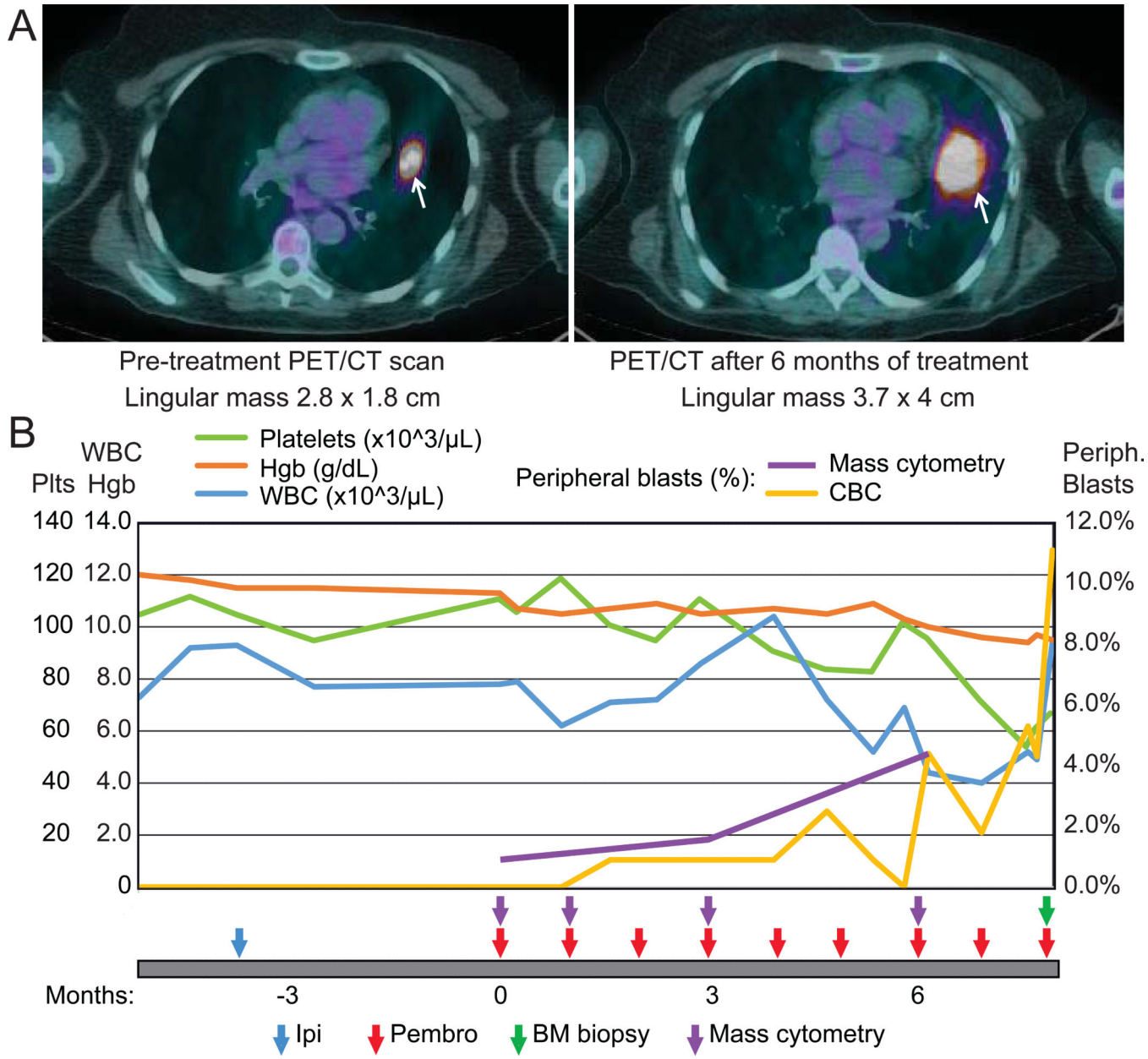

Figure 1. Clinical Imaging and Blood Counts

A) Pre-therapy and post-therapy PET/CT scans are shown that highlight a lingular metastasis that increases in size during the course of therapy. B) Select peripheral blood counts and blast cells by manual differential are shown prior to and during therapy. The patient had a pre-existing thrombocytopenia (green line) that worsened over time. After therapy initiation, blasts (yellow) are seen to increase as hemoglobin (Hgb, orange line) drops and white blood cells (blue line, same scale as Hgb) remain in the normal range. As of 9 months post therapy initiation, the patient remains on anti–PD-1 therapy.

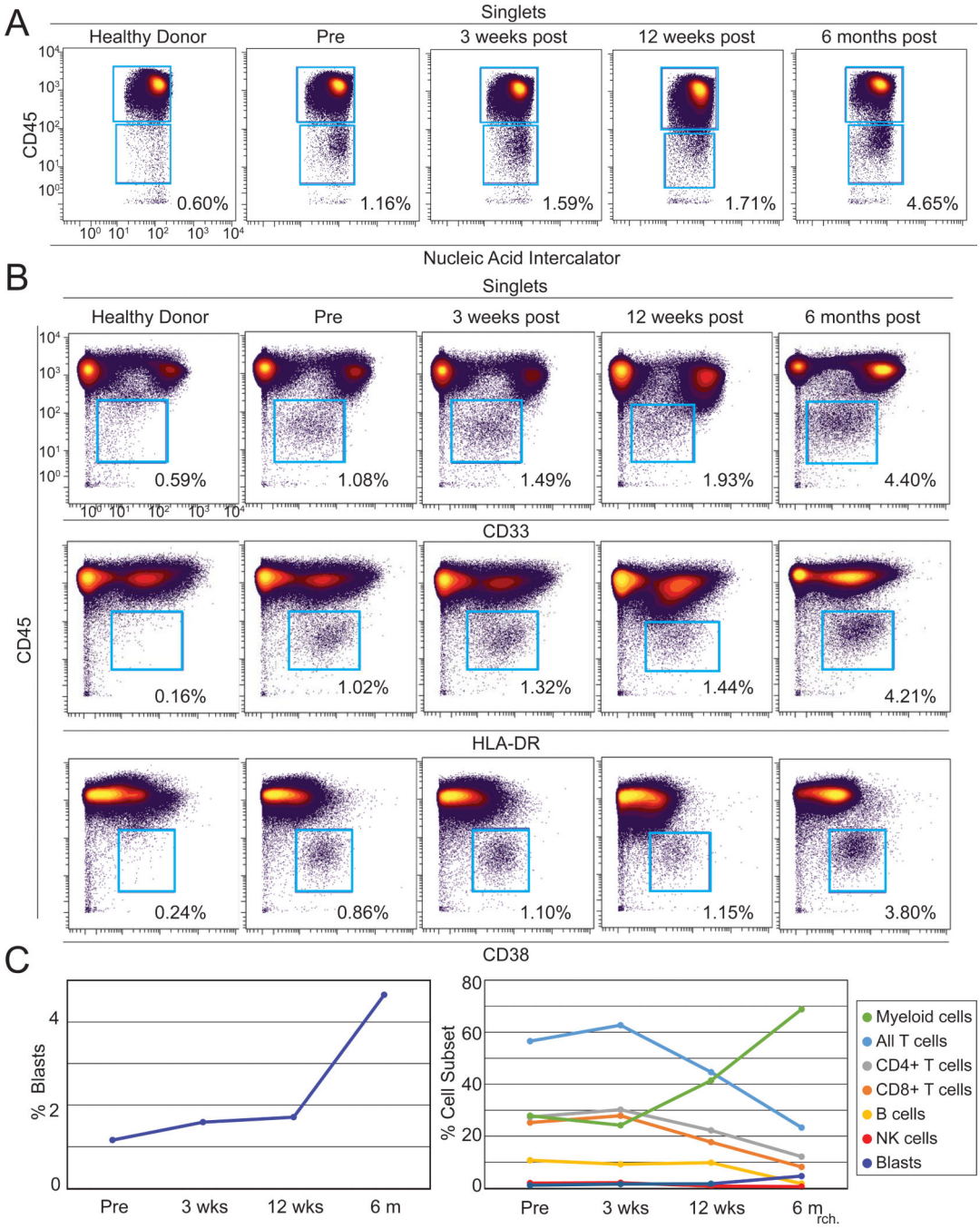

Figure 2. Identification of peripheral blasts by mass cytometry in a melanoma patient undergoing anti–PD-1 therapy

A 33 parameter mass cytometry panel was used to immunophenotype peripheral blood from a melanoma patient over the course of anti–PD-1 therapy. A) Cells positive for nucleic acid intercalator, a marker of nuclear DNA, and low for CD45 were identified over the course of therapy, but not in a healthy donor. B) The majority of $CD45^{lo}$ events (blue gate) from the patient expressed intermediate levels of CD33 and high levels of both HLA-DR and CD38 compared to non-blasts, consistent with peripheral myeloblast phenotype. C) Peripheral blasts increased from 1.16% to 4.65% of all PBMC (left). The percentage of T (light blue),

B (yellow), and NK (red) cells declined over the course of therapy while the percentage of myeloid cells (green) increased (right).

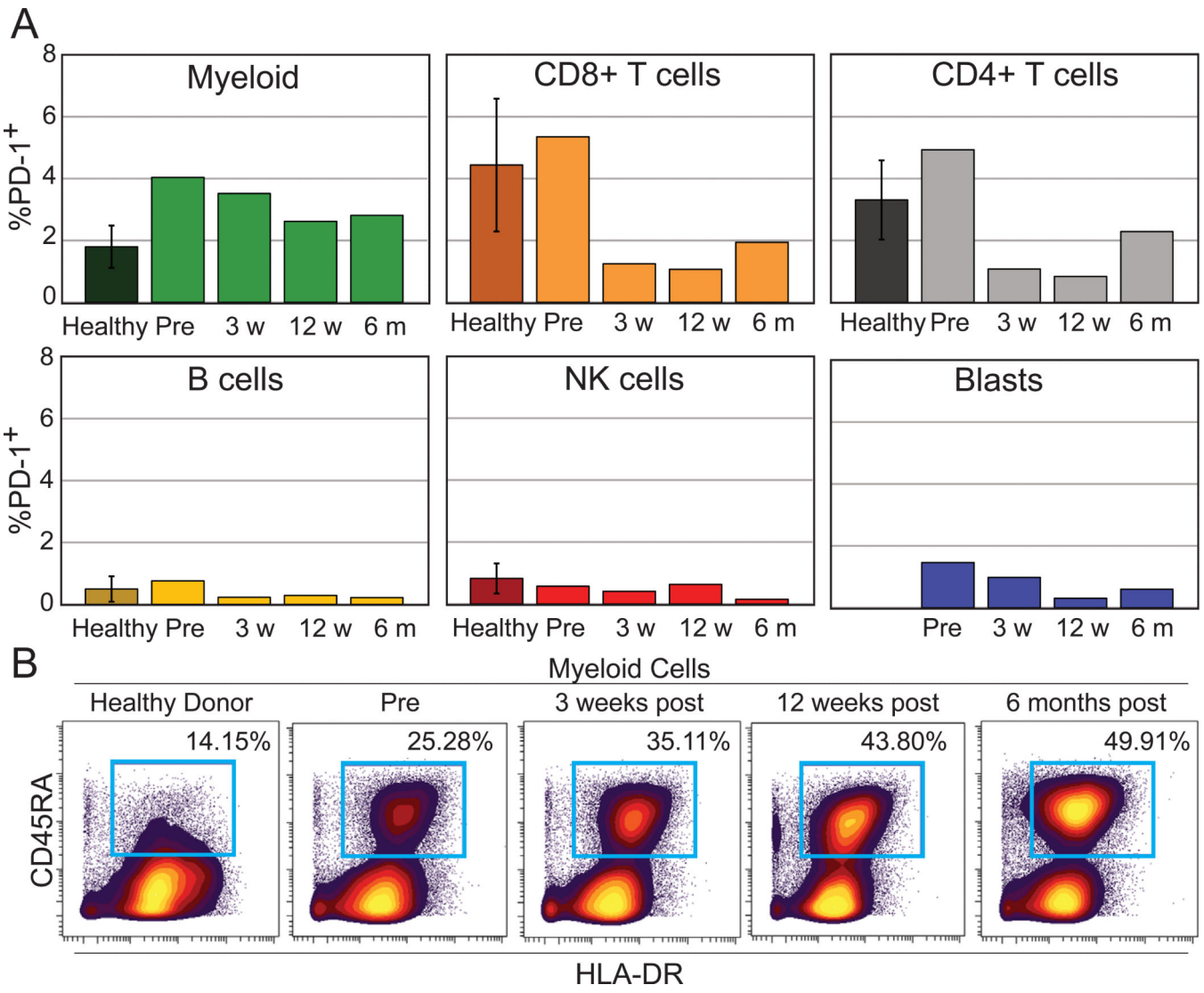

Figure 3. Frequency of PD-1$^+$ monocytes in this case remained higher during therapy than in untreated healthy controls

A) The percentage of PD-1$^+$ cells was determined for blasts, CD8 T cells, CD4 T cells, myeloid cells, NK cells, and B cells. For healthy, $n = 5$. B) Biaxial plots show the increase of activated monocytes through dual expression of CD45RA and HLA-DR on non-lymphoid cells from a healthy donor and from the patient over the course of anti–PD-1 therapy.

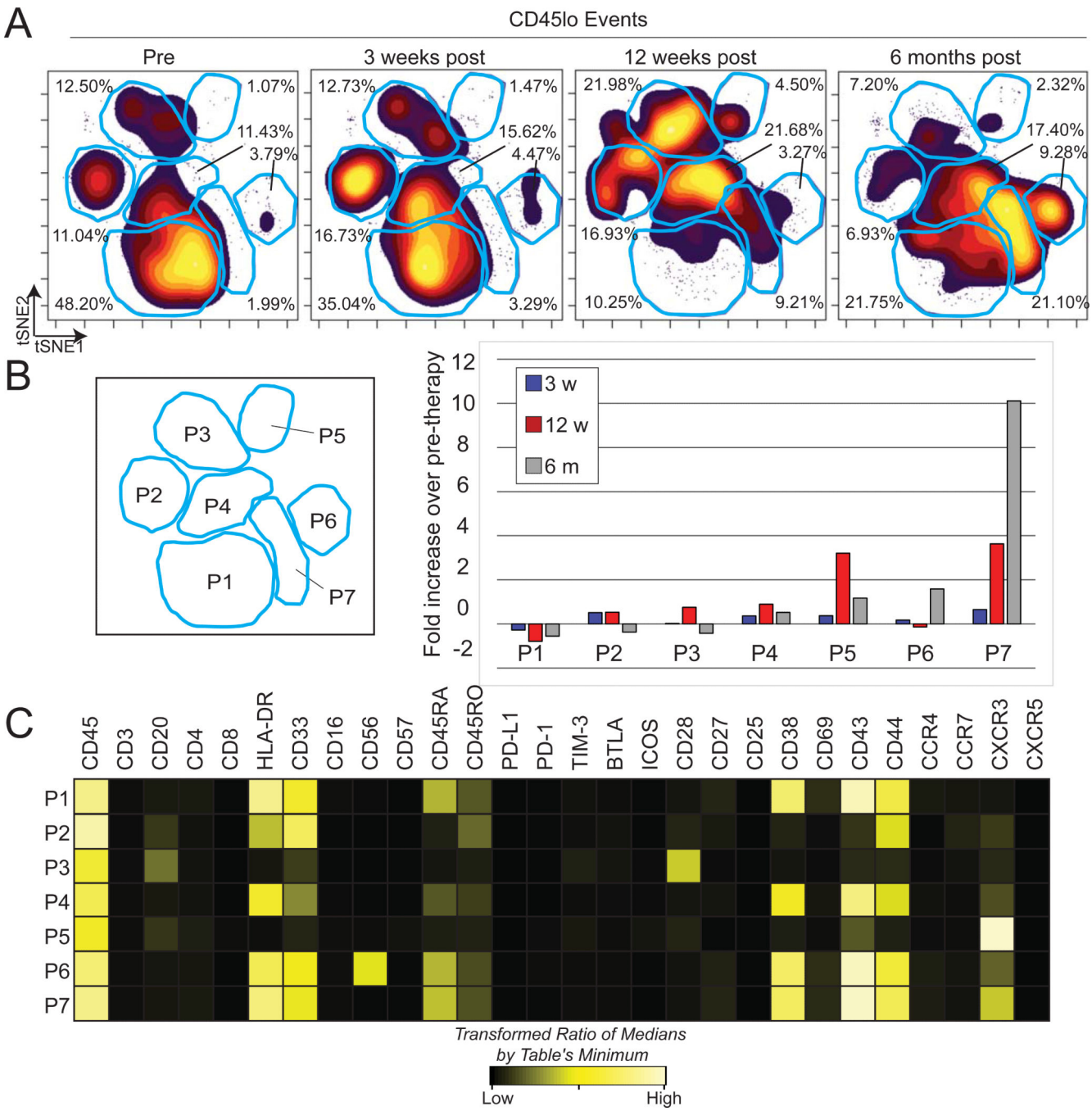

Figure 4. Peripheral blast phenotype shifts dramatically over the course of anti–PD-1 therapy

A) CD45lo events from the patient were gated and used to create a viSNE map. Blue gates identify major islands of cell density over all four time points. Each population denoted by the letter P followed by a number. B) Increase in cell density within each population (P, right) is shown as fold change over percentage of cells within sectors from the pre-therapy sample (left). C) A heatmap displays intensities of 28 measured proteins for each population

identified on the viSNE map. Intensity is shown as heat, calculated as a transformed ratio of medians by the table's minimum.